Ultramicroscopy 25 (1988) 155–164
North-Holland, Amsterdam



# SUPER-RESOLUTION IMAGING WITH NEAR-FIELD SCANNING OPTICAL MICROSCOPY (NSOM)

E. BETZIG, M. ISAACSON, H. BARSHATZKY, A. LEWIS and K. LIN

*School of Applied and Engineering Physics, Cornell University, Ithaca, New York 14853, USA*

Received 26 January 1988

Optical imaging with resolution exceeding the diffraction limit is demonstrated with near-field scanning optical microscopy (NSOM). The concept behind the technique and its experimental implementation is discussed. Images are presented which attest to its reproducibility and super-resolution capabilities. Although distinct, NSOM has technical features in common with scanning tunneling microscopy. However, since it is optically based it also shares many of the advantages of conventional optical microscopy, including non-destructiveness, speed, flexibility, and the ability to generate contrast in numerous ways.

## 1. Introduction

A completely new class of microscopies, scanned tip microscopies, have recently been developed for the characterization of surfaces on a microscopic scale. There is a fundamental principle which unifies the otherwise disparate scanned tip methods: the interaction between a sharp probe and a sample is used in a mechanical scanning arrangement to generate an image with the resolution being determined by a convolution of the probe diameter with the probe-to-sample separation.

The first such microscope to successfully address the challenges of probe formation, vibration isolation, micropositioning, and feedback was the Topografiner, a scanning field emission microscope invented by Young et al. [1]. This was the precursor to the scanning tunneling microscope (STM) [2]. By virtue of its atomic imaging capability, the STM represents the scanned tip technique which has received the most attention over the past several years, and it is discussed elsewhere in this issue. More recent scanned tip microscopies include scanning capacitance microscopy (SCM) [3], atomic force microscopy (AFM) [4–6], and scanning thermal profilometry (STP) [7]. The advantages and disadvantages of each technique are determined by the nature of the probe–sample interaction. Our contribution to scanned tip microscopy, near-field scanning optical microscopy (NSOM), is particularly promising because visible light has proven itself to be a remarkably versatile probe over the last several centuries. NSOM has the potential to combine the best aspects of conventional optical microscopy, scanning electron microscopy, and complementary scanned tip microscopies in terms of non-destructiveness, flexibility, speed and reliability.

The scanned tip used for NSOM consists of a subwavelength aperture in an optically opaque screen. An optical probe can be created by illuminating the aperture on the side opposite the sample (see fig. 1). If the screen is truly opaque, then the transmitted radiation is initially confined to the dimensions of the aperture, regardless of how small this may be. This occurs in the near field. In the far field, the radiation pattern rapidly diverges in a wavelength-dependent manner due to diffraction. To obtain a super-resolution image, a sample is placed within the near-field region relative to an illuminated aperture. The aperture then acts as a subwavelength-sized light source which can be scanned raster-fashion over the sample to generate an image. In addition to this illumination mode, collection-mode NSOM can be used as shown in the right side of fig. 2. In this case, super-resolution is also obtained since opti-

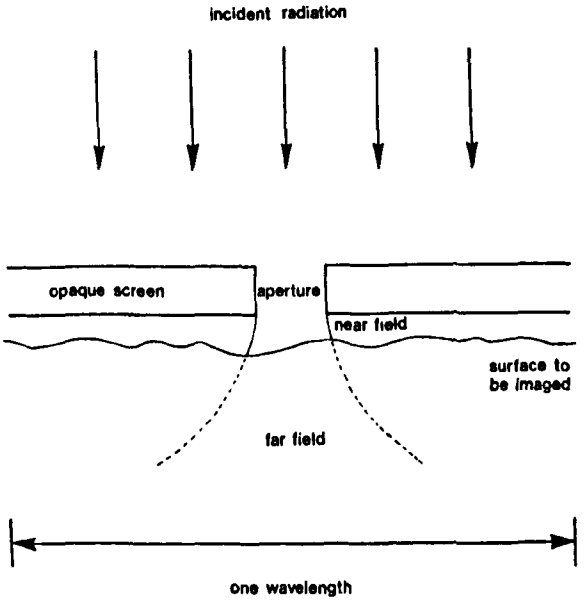


Fig. 1. Geometry for illumination-mode near-field scanning optical microscopy (NSOM).

cal information is collected from successive aperture-sized regions on a pixel-by-pixel basis. Finally, in reflection-mode NSOM, the aperture is used as both a transmitter and receiver.

The near-field concept was first described over thirty years ago by O'Keefe [8]. The experimental feasibility of the technique was first demonstrated at microwave frequencies (wavelength, $\lambda = 3$ cm) with a reflection instrument constructed by Ash and Nicholls (1972) [9]. The extension of the technique to the visible portion of the electromagnetic spectrum required the development of aperture fabrication and micropositioning techniques on a scale five orders of magnitude smaller than those used in the microwave region. Hence, over a decade passed before our first reports [10,11] on near-field optical imaging appeared. Since these initial publications, several other groups have worked on near-field imaging either with visible [12–15] or far infrared [16] wavelengths. In this paper, we consider only the development of NSOM at Cornell. For other methods, the reader is advised to refer to the literature.

## 2. NSOM design

The construction of an NSOM instrument is guided by two parameters: the degree to which light can be passed through a subwavelength aperture and the distance to which the near-field collimation extends. Over 40 years ago, Bethe [17] determined that, for a fixed incident intensity, the

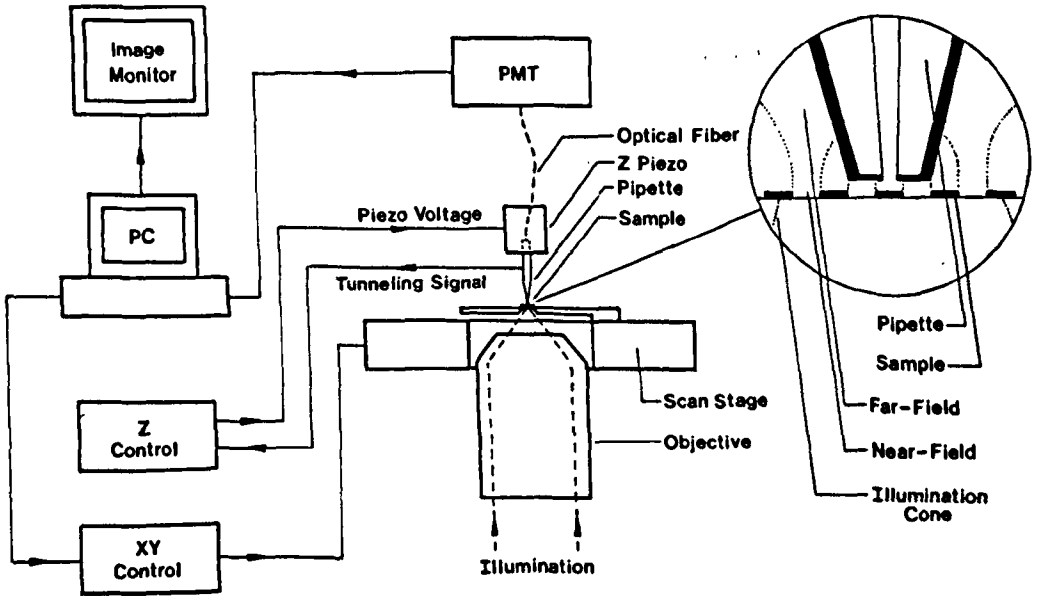


Fig. 2. Schematic for the collection-mode NSOM instrument (from ref. [25]).

power transmitted through a subwavelength aperture of radius $a$ in an infinitesimally thin screen decreases as the sixth power of $a$. The signal is further attenuated within a screen of finite thickness [18], since the aperture then behaves as a waveguide in which all modes are evanescent. Hence, low-light-level detectors are needed to obtain super-resolution without resorting to exhorbitant incident intensities. With respect to the collimation, we have used a rigorous model for diffraction by a narrow slit in a thick screen to determine that the near field extends roughly 200 Å from a 500 Å opening [19]. Furthermore, the intensity was found to decrease rapidly within the near field, so that the aperture sample separation must be maintained with $\leq 20$ Å accuracy to obtain 500 Å resolution. Similar results have been found for the case of a circular aperture [20]. Although these aperture–sample separation tolerances are not as stringent as the tip–sample separation in STM, these requirements must be met by application of similar technology.

The sensitivity of the probe–sample separation to external stimuli is minimized by a combination of microscope rigidity and vibration isolation, as in all scanned tip microscopies. In our NSOM instrument, rigidity was afforded by the choice of a compact cylindrical design constructed with stiff materials [21]. This design was also chosen to minimize the effects of thermal drift. Isolation from building disturbances was provided by a two-stage air table system, which in turn was surrounded by sound-absorbing curtains for acoustic isolation. Use of the instrument in a tunneling feedback mode demonstrated that the relative motion was reduced to 0.3 nm in a 1 kHz bandwidth from DC.

The single most important factor influencing NSOM design is the aperture fabrication process. We originally created apertures in a flat screen using electron beam lithography [11]. However, it is not only necessary to produce an aperture which is small with respect to optical wavelengths, but, because of the small extent of the near field, this

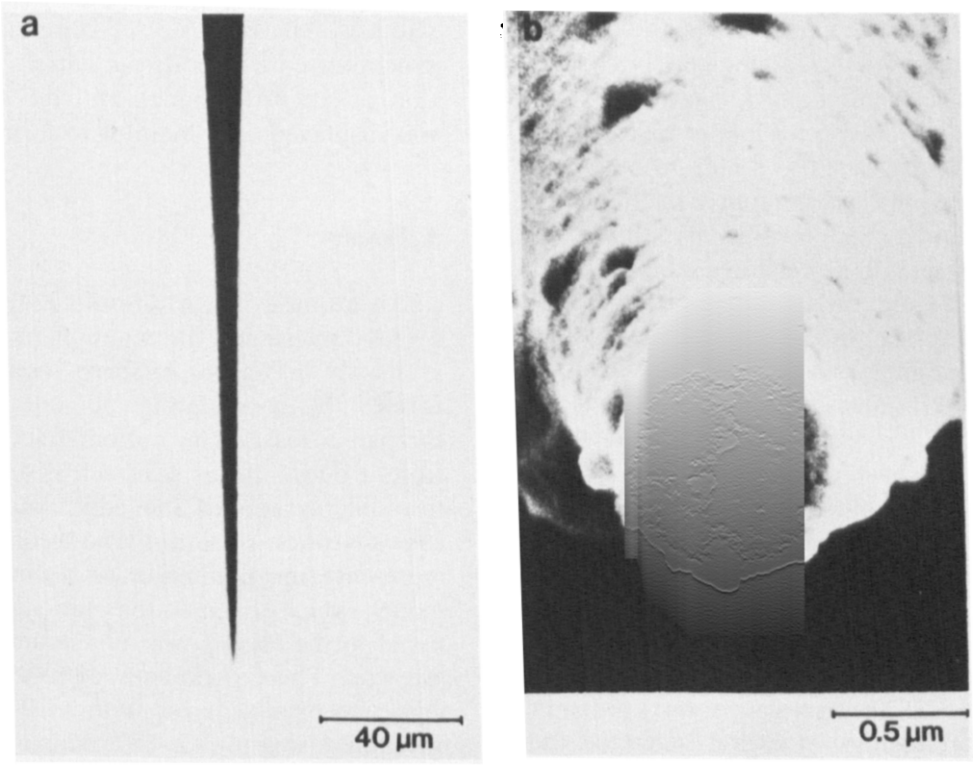


Fig. 3. Scanning electron micrographs of pipette apertures. (a) Low magnification side view of a pipette. (b) High magnification axial view demonstrating a 150 nm aperture.

aperture must be at the exact apex of a highly tapered probe to permit the imaging of relatively rough surfaces. We have accomplished both of these goals by pulling locally heated, hollow glass capillary tubes past the breaking point to produce sharply tapered micropipettes. Although this technique was originally applied to patch clamping in membrane biophysics [22], we have extended it for use in near-field microscopy [23–25]. The pipettes are evaporated on the sides with 200 nm of aluminum and on the tip with 50 nm to insure that light can be passed only through the central aperture. The side view of a pipette in fig. 3a demonstrates that the taper condition is satisfied. Fig. 3b shows a head-on view of a metallized pipette with an 800 nm outer diameter.

There are many advantages to the pipette method of aperture fabrication. First, the geometry allows for maximization of signal. The metallized pipette can be viewed as a conducting optical waveguide. If the outer diameter at the tip is kept above the cut-off value at optical frequencies, then the radiation is evanescent only within the region of the thin metal film at the tip which optically defines the aperture. Second, the method is extremely simple, so that pipettes can be formed both inexpensively and rapidly. Third, the technique is highly reproducible. Pipettes pulled under identical conditions vary by $< 20\%$ in outer and inner diameters, and yields approach 100%. Finally, the method is very flexible. By varying the heat, pulling force, pulling velocity and the amount and time of cooling with a commercial pipette puller [26], the outer and inner diameters, taper length, and taper angle can be drastically changed. We have produced outer diameters in the range of 30 nm to 30 $\mu$m and aperture diameters from 30 nm to 10 $\mu$m. Because of this flexibility, pipette technology may also prove useful in some of the scanned tip microscopes mentioned earlier.

Although our initial feasibility measurements [23,24] were performed with an NSOM prototype operating in the illumination mode, we have more recently demonstrated the collection mode system [25] shown in fig. 2. The new system was chosen in part because preliminary modeling suggested the collection mode may achieve better resolution, in part because luminescent samples could be directly imaged, and in part because the collection method could be combined with external illumination to form a reflection NSOM system. In this initial form of our instrument, illumination from a Xe arc lamp or a He–Ne laser was focused with either a microscope objective or a laser singlet onto the lower surface of a transparent sample. The transmitted light directly beneath an aperture was then collected in the near field and sent over an optical fiber to a photomultiplier tube for detection. The focusing objective also served as part of an inverted optical microscope to guide the lateral positioning of the pipette relative to the sample. Another microscope at a 30° angle to the plane of the sample was used for the initial vertical positioning. Coarse ($> 1$ $\mu$m) translation along all three axes was accomplished with velocity servo-controlled actuators. A piezoelectric tube was used for fine motion and feedback in the vertical direction. Two methods have been successfully used to generate the lateral scanning motion. With the bending tube system [27] the pipette is translated, whereas a commercial piezoelectric stage [28] is employed when the sample is scanned. An IBM PC/AT computer was used to synchronize the lateral scan pattern to the digitization of the PMT signal, and the combined data was displayed on a monitor to form an image.

## 3. Results

An example of early results [24] obtained with a one-dimensional illumination mode instrument is shown in fig. 4. A sharp, opaque edge was formed by evaporating 50 nm of chromium through a mask. The bottom trace was obtained from a densitometer scan across a scanning electron micrograph of the edge, and indicates an edge sharpness of 30 nm. The second lowest curve represents the prediction of a simple near-field model, which assumes that the signal is proportional to the third power of the unoccluded aperture area. The experimental data superimposed on this curve was acquired with a 100 nm diameter aperture. Using the 12–88% points as a guide, the NSOM edge sharpness is 60 nm. The upper two curves show the edge sharpness calculated from

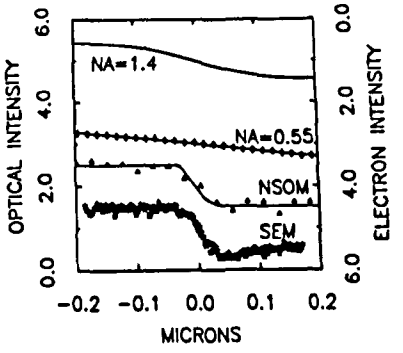


Fig. 4. Comparison of edge sharpness obtained with scanning electron microscopy, illumination-mode NSOM, and conventional optical microscopy with two different numerical apertures (from ref. [24]).

the theory for an incoherent scanning optical microscope (SOM) assuming objective numerical apertures of 0.55 and 1.4. The data on the one curve was obtained with the same 0.55 NA objective used to collect the signal in the NSOM prototype. Clearly, the edge sharpness in the near-field case is much closer to the SEM case than either of the other situations. Furthermore, the theoretical curve for the 1.4 NA SOM arrangement approaches the best obtainable resolution for conventional optical microscopy, yet the NSOM sharpness is clearly superior. Other scans taken with this instrument [24] have demonstrated that fluorescence NSOM with sub-100 nm resolution is obtainable. This result has important implications for the application of the technique to biology and polymer science.

Our collection-mode images [25] were recorded in any one of three different submodes, which are distinguished by the method with which the pipette is brought to the surface and maintained within the near field. In the tunneling mode, the relative aperture-sample separation is held fixed by applying a bias voltage to the tip or sample and monitoring the resulting tunneling current exactly as in an STM. There are several disadvantages of this method for our immediate application. First, the pipette and sample must be coated with about 20 nm of gold to insure conductivity. Second, the separation required to obtain a measurable tunneling current (~ 5 Å) is much smaller than that required for near-field imaging (~ 200 Å), so that the speed is limited by the feedback mechanism rather than by the optical response time. Lastly and most seriously, the images obtained thus far with this mode have usually been marred by the presence of streaks in the scan direction. These may result when the pipette is forced to push through locally adsorbed insulators to maintain the tunneling current or may be due to the fact that the pipette drags due to a combination of its weak spring constant and the strong electrostatic interaction with the surface occasioned at typical tunneling distances.

In the constant-height mode, the pipette is first optically positioned above the sample. Scans are then generated at successively closer distances without the use of any feedback. Approach to the near field is evidenced by a gradual increase of resolution in the resulting images, and contact is determined when the images become distorted. The speed is limited only by the strength of the near-field optical signal and in general can be quite rapid. Furthermore, with the constant height mode it is possible to map the evolution of diffraction by the sample from the near to the far field. The disadvantage of the method is that only samples which are flat on the scale of the near field can be imaged with high resolution at all points. In addition, the initial approach must proceed cautiously, because the image quality changes rapidly only within the small near-field region.

The contact mode represents a synthesis of the above two methods. A tunneling current is monitored while the pipette advances toward the surface, but is not used for feedback during the scanning process. The speed of initial approach characteristic of the tunneling mode is then retained along with the fast scanning capability of the constant height mode. Although this method virtually assures that the pipette and sample will occasionally meet, the contact force is sufficiently low and the pipette sufficiently flexible so that most images are not distorted and neither the probe nor sample are damaged. Unfortunately, the method is still limited to flat samples on flat regions on a rough surface.

To respond to the limitations of these methods, we are developing a feedback mechanism based on capacitance microscopy [3]. This system should allow for a rapid initial approach, fast scanning, a

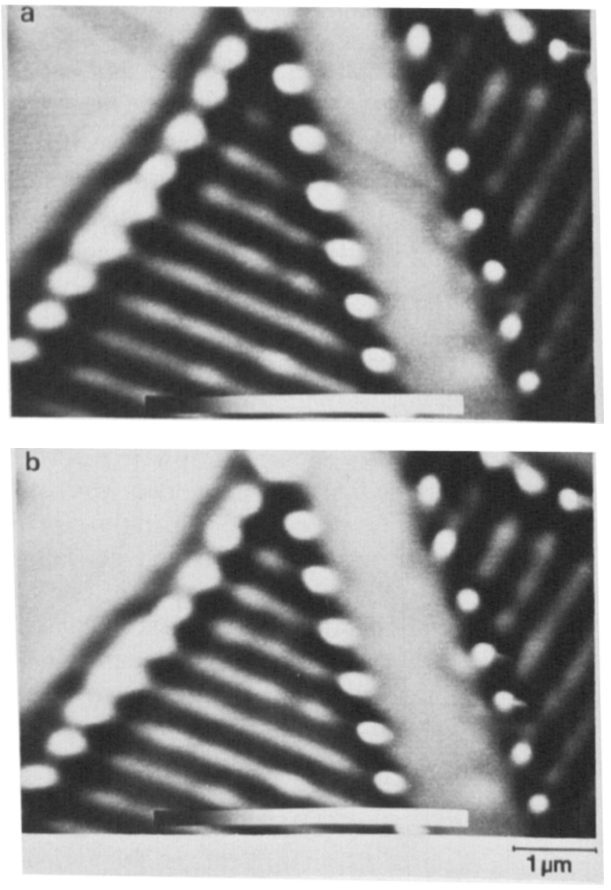


Fig. 5. (a) A scanning electron micrograph of a test pattern. (b) A collection-mode NSOM micrograph of a similar pattern. From ref. [25].

broad range over which feedback is possible, and adjustability of the relative aperture–sample separation within this range.

To assess quantitatively the resolution of any microscope, it is necessary to image well-characterized test structures. For our collection-mode NSOM instrument, these structures were comprised of opaque aluminum patterns resting on a transparent membrane of $Si_3N_4$. The patterns were created using electron beam lithography [29] combined with a metal lift-off procedure. A representative sample, shown in the scanning electron micrograph of fig. 5a, consisted of two perpendicular gratings with 0.25 $\mu$m wide lines and spaces. 1000 Å of aluminum was evaporated to form the lines, which had typical edge sharpnesses of 200 Å. A near-field scanning optical micrograph obtained in the contact mode of a similar sample is presented in fig. 5b. The opaque aluminum lines appear as black stripes. For this and later images, a signal of $\approx 2$ pW was measured when a pipette similar to that shown in fig. 2 was used. Complete $512 \times 512$ pixel images over $7.5 \times 7.5$ $\mu$m could then be captured within 10 min. This time can be decreased by more than an order of magnitude using a more efficient illumination system. All the lines are easily resolved, so that the Rayleigh resolution is clearly better than 0.25 $\mu$m. If one closely inspects such images, one finds the reproduction of finer features of the pattern clearly extends to an even smaller scale. Again using the 12–88% detected power points as a criterion, an average edge sharpness of 120 nm is indicated, and a sharpness of 70 nm can be obtained at certain regions within the lines. The assumed aper-

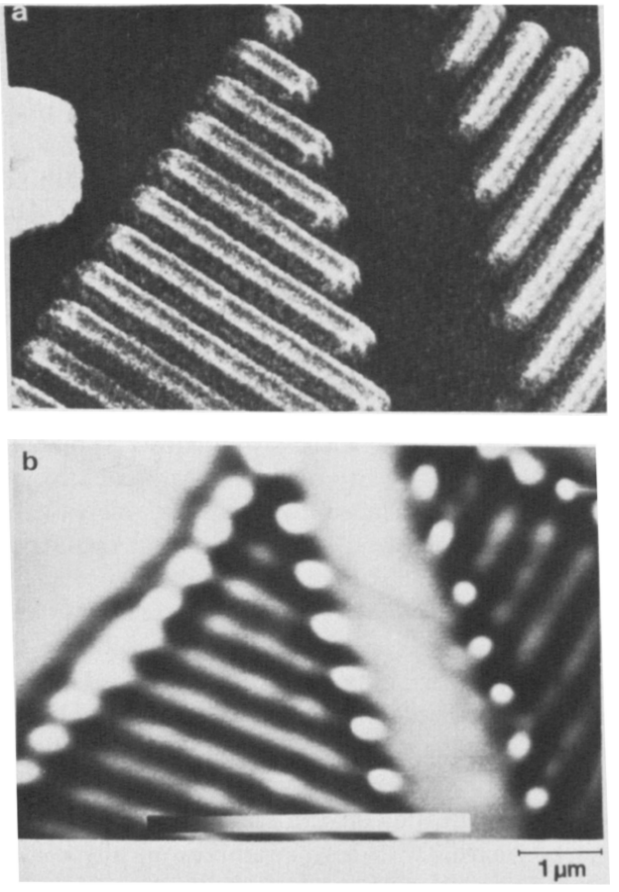


Fig. 6. Reproducibility of the collection-mode instrument is demonstrated in two images of the same pattern. From ref. [25].

ture size of 150 nm is completely consistent with these values, since the assumption of $a^6$ transmission dependence leads to a predicted maximum edge sharpness of 63 nm.

The reproducibility of our NSOM imaging is shown in fig. 6. Here we show two successive NSOM images of the same grating taken in the contact mode. These images are almost indistinguishable, and yield the same average and peak values of edge sharpness. That this result was obtained in the contact mode is especially encouraging, since it demonstrates that gentle contact is nondestructive to the pipette and sample alike. Indeed, we have found no limit to the number of such images which can be generated with a single pipette. The stability, mechanical flexibility, and durability of pipettes represent several more advantages to their use in near field microscopy.

There are two particularly interesting types of features in fig. 6. First, in the upper-right-hand corner of both fig. 6a and fig. 6b there is a streak in the scan direction arising from the pipette dragging across the surface during contact. Two smaller streaks apparent in the right-hand side of fig. 6b which are not present in fig. 6a presumably result from a drift in the vertical pipette position between scans. Second, both images display a series of bright transmission peaks positioned between each pair of lines and at their joint endpoints. Originally it was thought that these might be due to intense near-field scattering at the highly conductive and sharp aluminum corners. However, the fact that these features do not appear in scans of non-periodic patterns (see fig. 8) suggests that this may not be true. A further clue to these anomalous bright regions is afforded by the observation that the maximum value within each peak is approximately twice the level obtained over the transparent membrane away from the grating.

By the nature of the NSOM method, it is clear that within the near field, the resolution is determined solely by the aperture size. However, as the aperture–sample separation increases, the res-

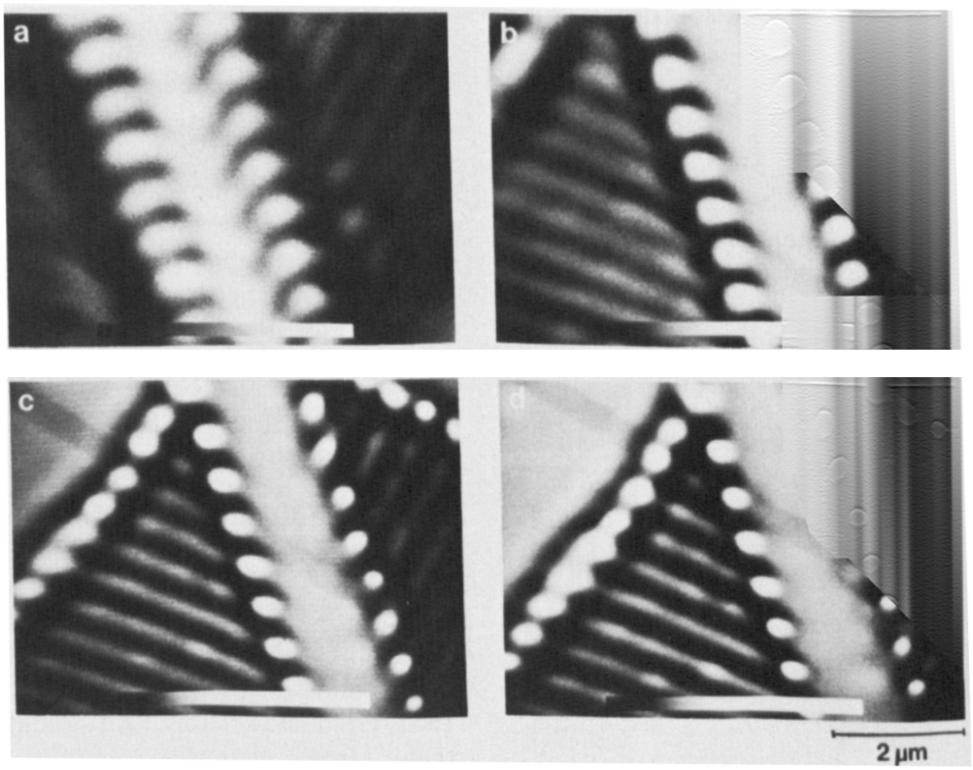


Fig. 7. The effect of the aperture–sample separation on resolution is shown for separations of (a) 780 nm, (b) 330 nm, (c) 150 nm, and (d) in contact. From ref. [25].

olution becomes a function of both the separation and aperture size. To document this transition, we have performed several scans at various separation distances as shown in fig. 7. At the distance of 780 nm in fig. 7a, the resolution is apparently dominated by the separation, since the grating is not well resolved. The distance of 330 nm in fig. 7b is similar to the line separation of 250 nm within the grating. Hence, we expect, and find, that individual lines can be seen, although not sharply. Fig. 7c, where the separation is equal to the presumed aperture size of 150 nm, demonstrates only slightly poorer resolution than the contact-mode scan in fig. 7d. These two images confirm our initial theoretical analysis: the near-field resolution and extent are both determined by the aperture size independent of the wavelength. Further verification of these observations has been obtained by repetition of the experiment with a different aperture size [25].

One of our current goals is to determine the fundamental and practical limits to the resolution in NSOM. Although apertures as small as 300 Å can be made easily, the finite opacity of real metal films suggests that insufficient aperture–screen contrast may exist for apertures below 500 Å [19]. To test this hypothesis, we recently created samples with test structures of all sizes down to the 500 Å level. An NSOM image of an intermediate-sized structure from one such sample is shown in fig. 8. We hope that these samples will allow us to determine the effective modulation transfer function of the NSOM system and assess the ultimate resolution capabilities of the method.

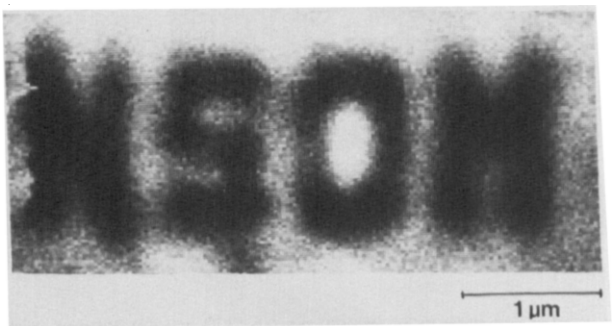


Fig. 8. NSOM micrograph of a newer, non-periodic pattern.

## 4. Conclusions

The results presented above clearly demonstrate that near-field scanning optical microscopy can be used to extend optical imaging well beyond the conventional limit imposed by diffraction. Experimental implementation of NSOM involves application of much of the same technology as developed for other scanned tip microscopies such as tunneling microscopy. The use of pipette-type apertures for NSOM has been shown to be advantageous for numerous reasons. The reproducibility of the technique has been demonstrated, and the resolution has been shown to conform qualitatively with theoretical predictions.

In the growing list of microscopic methods, near-field microscopy appears particularly promising. The resolution is superior to that of conventional optical microscopy, yet, in contrast with scanning electron microscopy, the technique is almost completely non-destructive. Among the various scanned tip microscopies, visible light represents a particularly useful probe. Optical detectors can be made sensitive over an enormous range down to the photon-counting level, so that NSOM is potentially fast, non-destructive, and sensitive to minute changes in optical properties. Furthermore, optical detection is flexible, as is evidenced by the popularity of polarized light and phase contrast microscopy, and the growth of numerous spectroscopic techniques. In particular, because of its demonstrated ability to be used for fluorescence microscopy, NSOM shows great promise for the in vivo imaging of biological specimens at high resolution [23,30].

## Acknowledgements

We wish to thank John Koumjian for his contributions. This work is supported by NSF contract ECS-8410304 and US Air Force contract AFOSR-84-0314. Test patterns were fabricated at the National Nanofabrication Facility at Cornell (NSF grant ECS-8619040). E.B. is supported as an IBM Graduate Fellow. We would also like to thank Dr. W. Baumeister and Dr. E. Zeitler for their invitation to participate in this collection of articles on scanned tip microscopes.

## References


[1] R. Young, J. Ward and F. Scire, Rev. Sci. Instr. 43 (1972) 999.

[2] G. Binnig, H. Rohrer, Ch. Gerber and E. Weibel, Phys. Rev. Letters 49 (1982) 57.

[3] J.R. Matey and J. Blanc, J. Appl. Phys. 57 (1986) 1437.

[4] G. Binnig, C.F. Quate and Ch. Gerber, Phys. Rev. Letters 56 (1986) 930.

[5] Y. Martin, C.C. Williams and H.K. Wickramasinghe, J. Appl. Phys. 61 (1987) 4723.

[6] J.R. Albtecht and C.F. Quate, J. Appl. Phys. 62 (1987) 2599.

[7] C.C. Williams and H.K. Wickramasinghe, Appl. Phys. Letters 49 (1986) 1587.

[8] J.A. O'Keefe, J. Opt. Soc. Am. 46 (1956) 359.

[9] E.A. Ash and G. Nicholls, Nature 237 (1972) 510.

[10] A. Lewis, M. Isaacson, A. Muray and A. Harootunian, Biophys. J. 41 (1983) 405a.

[11] A. Lewis, M. Isaacson, A. Harootunian and A. Muray, Ultramicroscopy 13 (1984) 227.

[12] D.W. Pohl, W. Denk and M. Lanz, Appl. Phys. Letters 44 (1984) 651.

[13] U.Ch. Fischer, J. Vacuum Sci. Technol. B3 (1985) 386.

[14] U. Durig, D.W. Pohl and F. Rohner, J. Appl. Phys. 59 (1986) 3318.

[15] U.Ch. Fischer, J. Opt. Soc. Am. B3 (1986) 1239.

[16] G.A. Massey, J.A. Davis, S.M. Katnik and E. Omon, Appl. Opt. 24 (1985) 1498.

[17] H.A. Bethe, Phys. Rev. 66 (1944) 163.

[18] A. Roberts, J. Opt. Soc. Am. A4 (1987) 1970.

[19] E. Betzig, A. Harootunian, A. Lewis and M. Isaacson, Appl. Opt. 25 (1986) 1890.

[20] Y. Leviatan, J. Appl. Phys. 60 (1986) 1577.

[21] E. Betzig, PhD Dissertation, Cornell University (1988).

[22] B. Sakmann and E. Neher, Eds., Single Channel Recording (Plenum, New York, NY, 1983).

[23] E. Betzig, A. Lewis, A. Harootunian, M. Isaacson and E. Kratschmer, Biophys. J. 49 (1986) 269.

[24] A. Harootunian, E. Betzig, M. Isaacson and A. Lewis, Appl. Phys. Letters 49 (1986) 674.

[25] E. Betzig, M. Isaacson and A. Lewis, Appl. Phys. Letters 51 (1987) 2088.

[26] Sutter Instruments model P80-PC, San Rafael, CA, USA.

[27] G. Binnig and D.P.E. Smith, Rev. Sci. Instr. 57 (1986) 1688.

[28] F.E. Scire and E.C. Teague, Rev. Sci. Instr. 49 (1978) 1735.

[29] M. Isaacson, A. Muray, M. Scheinfein, I. Adesida and E. Kratschmer, Microelectron. Eng. 2 (1984) 58.

[30] A. Lewis, E. Betzig, A. Harootunian, M. Isaacson and E. Kratschmer, in: Spectroscopic Membrane Probes, Ed. L. Loew (CRC Press, Cleveland, OH, in press).